JACS
JOURNAL OF THE AMERICAN CHEMICAL SOCIETY
Communication
pubs.acs.org/JACS

A New Deep-Ultraviolet Transparent Orthophosphate $LiCs_2PO_4$ with Large Second Harmonic Generation Response

Lin Li,[†,‡,∥] Ying Wang,[†,∥] Bing-Hua Lei,[†,‡] Shujuan Han,[†] Zhihua Yang,[†] Kenneth R. Poeppelmeier,[*,§] and Shilie Pan[*,†]

[†]Key Laboratory of Functional Materials and Devices for Special Environments of CAS, Xinjiang Key Laboratory of Electronic Information Materials and Devices, Xinjiang Technical Institute of Physics & Chemistry of CAS, 40-1 South Beijing Road, Urumqi 830011, China

[‡]University of Chinese Academy of Sciences, Beijing 100049, China

[§]Department of Chemistry, Northwestern University, 2145 Sheridan Road, Evanston, Illinois 60208-3113, United States

Supporting Information

ABSTRACT: $LiCs_2PO_4$, a new deep-ultraviolet (UV) transparent material, was synthesized by the flux method. The material contains unusual edge-sharing LiO_4-PO_4 tetrahedra. It exhibits a very short absorption edge of λ = 174 nm and generates the largest powder second harmonic generation (SHG) response for deep-UV phosphates that do not contain additional anionic groups, i.e., 2.6 times that of KH_2PO_4 (KDP). First-principles electronic structure analyses confirm the experimental results and suggest that the strong SHG response may originate from the aligned nonbonding O-2p orbitals. The discovery and characterization of $LiCs_2PO_4$ provide a new insight into the structure−property relationships of phosphate-based nonlinear optical materials with large SHG responses and short absorption edges.

Nonlinear optical (NLO) materials, particularly for deep-ultraviolet (UV) applications, have provoked considerable interest owing to their promising applications in laser and photonic technologies.[1] Up to now, only $KBe_2BO_3F_2$ and $RbBe_2BO_3F_2$ can generate deep-UV coherent light wavelengths below 200 nm by direct second harmonic generation (SHG).[1a] However, the strong layering tendency limits their practical application. Hence, the exploration and development of the next generation deep-UV NLO materials are in great demand. Yet, exploration of suitable deep-UV NLO materials that possess relatively large SHG response, wide deep-UV transparent window, and phase matching ability is a serious materials discovery challenge.[1c] To date, new potential deep-UV NLO materials are mostly limited to borates, such as $NaSr_3Be_3B_3O_9F_4$,[2] $Ba_4B_{11}O_{20}F$,[3] $Cs_2SiB_4O_9$,[4] $Li_4Sr(BO_3)_2$,[5] $Rb_3Al_3B_3O_{10}F$,[6] and $K_3Ba_3Li_2Al_4B_6O_{20}F$.[7]

Beyond borates, leading by the discovery of $Ba_3P_3O_{10}X$ (X = Cl, Br),[8] a new thought of finding deep-UV NLO materials in phosphates has recently been proposed. Compared with borates, phosphates exclusively contain asymmetric PO_4 tetrahedra as building units, and they usually exhibit short UV cutoff edges. However, phosphates suffer from their own drawback: the microscopic second-order nonlinear susceptibility of the PO_4 units is 1 order of magnitude smaller than that of the planar B−O groups, BO_3 and B_3O_6. As such, the SHG coefficients of phosphates are relatively small.[1] Notably, phosphates containing additional B−O groups, i.e., borophosphate or borate-phosphate, can exhibit relatively large SHG responses, e.g., BPO_4 (2 × KH_2PO_4, KDP),[9] $MBPO_5$ (M = Sr, Ba) (∼1 × KDP),[10] and recently discovered $Ba_3(ZnB_5O_{10})PO_4$ (4 × KDP).[11] However, they are not simple phosphates, and their SHG effect is closely related to the introduced B−O groups. Generally, SHG responses of phosphates can be enhanced by introducing additional distortive structural units, such as d^0 transition metal cations susceptible to second-order Jahn−Teller (SOJT) effect (Ti^{4+}, Nb^{5+}, Mo^{6+}, etc.),[12] cations with stereoactive lone pairs (Pb^{2+}, Bi^{3+}, Te^{4+}, etc.),[13] or d^{10} cations that undergo an off-center displacement (Zn^{2+} and Cd^{2+}).[11,14] Yu et al. recently introduced all these three types of structural units into a family of phosphate materials which exhibit strong SHG responses ranging from 2.8 to 13.5 × KDP.[13b,c] However, employing these strategies in phosphates will also cause an unwanted red-shift in the absorption edge, that hinders the application in the deep-UV.

In order to enhance the SHG response of phosphates while also retaining the deep-UV transparency, other structural design strategies have been put forward. For example, the pioneering work by Yu et al. took advantage of the asymmetric C_1-$P_3O_{10}^{5-}$ building units leading to the good NLO properties of $Ba_3P_3O_{10}X$ (X = Cl, Br).[8] Zhao et al. developed an approach based on the use of flexible $P_3O_{10}^{5-}$ building units in $Ba_5P_6O_{20}$.[15] They also suggested that polymerization of P−O groups may help to increase the distortion of PO_4 tetrahedra, as represented by $RbBa_2(PO_3)_5$.[16] It is noted that these compounds are all polyphosphates and that the polymerized P−O groups are necessary for SHG enhancement. Until now, there has not been an example of deep-UV transparent orthophosphates, namely, phosphates with isolated PO_4 tetrahedra, exhibiting large SHG responses (>1 × KDP). Here, we describe a new orthophosphate, $LiCs_2PO_4$, possessing an unusual edge-sharing LiO_4-PO_4 tetrahedra connectivity. A record SHG response of 2.6 × KDP under 1064 nm radiation is observed. This is quite unusual as $LiCs_2PO_4$ does not contain additional anionic groups, and the

Received: June 13, 2016
Published: July 12, 2016

DOI: 10.1021/jacs.6b06053
J. Am. Chem. Soc. 2016, 138, 9101−9104

SHG response cannot be fully explained by the traditional anionic group concept.[17]

Pure and polycrystalline $LiCs_2PO_4$ was synthesized via conventional solid-state techniques, and the phase purity was confirmed by powder XRD diffraction studies (Figure S1). Centimeter-size crystals of $LiCs_2PO_4$ were obtained utilizing a Li_2CO_3 self-flux (Figure 1a). $LiCs_2PO_4$ crystallizes in the

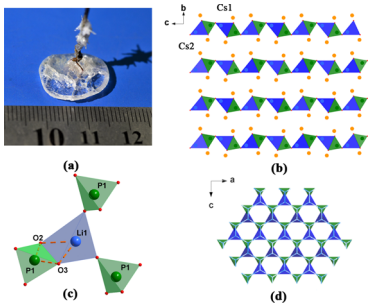

Figure 1. Macroscopic and atomic scale structure of $LiCs_2PO_4$. (a) Photo of 15 × 14 × 4 single crystal. (b) The 3D framework with Cs−O bonds omitted viewing along the *a*-axis. (c) Coordination environment of the LiO_4 tetrahedra. (d) The 6^3 net (white sticks) of 2D $(LiPO_4)^{2-}$ layer. LiO_4 (blue) and PO_4 (green) groups are viewed as two kinds of 4-connected nodes.

noncentrosymmetric and polar space group of $Cmc2_1$ (no. 36). The crystal structure may be described as two-dimensional (2D) $(LiPO_4)^{2-}$ layers along the *a* axis with the Cs^+ cations residing between the layers (Figure 1b). The P atom is tetrahedrally coordinated to oxygen atoms, generating the PO_4 tetrahedra with P−O bond lengths varying from 1.545(4) to 1.559(7) Å. The Li atoms form distorted LiO_4 tetrahedral structures with Li−O bond lengths ranging from 1.903(10) to 2.076(17) Å. Each LiO_4 tetrahedron is connected through one edge and two corners with the PO_4 tetrahedra (Figure 1c). These groups are connected forming a 2D $(LiPO_4)^{2-}$ layer (Figure 1d). Topologically, both LiO_4 and PO_4 tetrahedra can be viewed as 4-connected nodes, and the topology of the 2D layer can be described as a Shubnikov hexagonal plane net[18] with Schläfli notation[19] of (6^3) (Figure 1d). Additionally, the two unique Cs atoms are both 8-coordinate and form distorted CsO_8 polyhedra with the Cs−O bond lengths ranging from 3.004(7) to 3.695(5) Å. Bond valence calculations[20] (Li, 1.02; Cs, 1.04−1.12; P, 4.78; O, 1.82−2.08) indicate that the all atoms are in their normal oxidation states.

From a structural point of view, $LiCs_2PO_4$ differs from recently reported deep-UV NLO-active phosphates, such as $Ba_3P_3O_{10}X$ (X = Cl, Br),[8] $Ba_5P_6O_{20}$,[15] $RbBa_2(PO_3)_5$,[16] and $ALa(PO_3)_4$ (A = K, Cs),[21] in two aspects. First, $LiCs_2PO_4$ is an orthophosphate with isolated PO_4 tetrahedra, whereas the others are polyphosphates containing polymerized P−O groups (Table 1), such as $[P_2O_7]$ dimers, $[P_3O_{10}]$ trimers, and $[PO_3]^\infty$ chains. Second, it is noteworthy that a special Li1−O2−P1−O3 ring, that is an edge-sharing LiO_4-PO_4 configuration, is found in $LiCs_2PO_4$ (Figure 1c). According to the third rule of Pauling, except for some very special situations, the edge-sharing of tetrahedral units is often avoided in crystal structures.[22] In $LiCs_2PO_4$, the Li···P interatomic distance within the Li1−O2−P1−O3 ring is 2.59 Å, which is significantly larger than the ionic radii sum of Li and P ions. Thus, the cation−cation electrostatic repulsions are relatively small so that the influence on the stability of the ionic structure is not obvious. However, to our best knowledge,

Table 1. Optical and Structural Properties for Deep-UV NLO Phosphates

material	P−O groups	cutoff edge (nm)	SHG response (× KDP)
$LiCs_2PO_4$		174	2.6[b]
$LiCaPO_4$[25]	isolated $[PO_4]$	−[a]	0.2[b]
$LiNa_5(PO_4)_2$[26]		−[a]	0.3[b]
$Rb_2Ba_3(P_2O_7)_2$[16]	$[P_2O_7]$ dimer	<200	0.3
$Cs_2Ba_3(P_2O_7)_2$[27]		<176	weak
$Ba_3P_3O_{10}Cl$[8]		180	0.6
$Ba_3P_3O_{10}Br$[8]	$[P_3O_{10}]$ trimer	<200	0.5
$Ba_5P_6O_{20}$[15]		167	0.8
$CsLa(PO_3)_4$[21a]		167	0.5
$KLa(PO_3)_4$[21b]	$[PO_3]^\infty$ chain	162	0.7
$RbBa_2(PO_3)_5$[16]		163	1.4 (1.5[b])

[a]Indicates not reported. [b]Estimated from powder SHG data in this work.

such an example of edge-sharing LiO_4-PO_4 tetrahedra is first observed in $LiCs_2PO_4$.[23]

Motivated by the unusual structural feature and polar space group of $LiCs_2PO_4$, we measured its powder SHG properties under dry conditions. The curves of the SHG signals as a function of particle size were recorded using KDP as reference. As shown in Figure 2a, the SHG intensity of $LiCs_2PO_4$ increases with

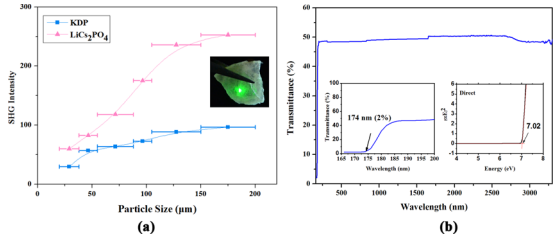

Figure 2. Linear and nonlinear optical properties of $LiCs_2PO_4$. (a) Phase-matching curves. Lines are guide for the eye. The inset presents the green SHG output light when a bulk single crystal irradiated by 1064 nm laser. (b) The UV optical transmittance spectrum on single crystal. The inners present the cutoff edge (left) and the corresponding band gap (right).

increasing particle size, which is consistent with type-I phase-matching behavior.[24] The inset of Figure 2a also demonstrates green SHG output light from bulk single crystal of $LiCs_2PO_4$, which further confirms its phase-matching ability at fundamental wavelength of 1064 nm. In the particle size range of 105−150 μm, $LiCs_2PO_4$ exhibits a SHG response of 2.6 × KDP (Figure 2a). In comparison, we recorded the SHG responses of NLO-active $RbBa_2(PO_3)_5$,[16] $LiCaPO_4$,[25] and $LiNa_5(PO_4)_2$[26] under the same experimental condition (Table 1). $RbBa_2(PO_3)_5$ was previously thought to be the one possessing the "largest" SHG response of 1.4 × KDP (~1.5 × KDP according to our results) among all deep-UV NLO phosphates.[16] Remarkably, $LiCs_2PO_4$ has an even larger SHG response, and it is 1.7 times that of $RbBa_2(PO_3)_5$. It is also interesting to see that the other two NLO-active orthophosphates only show very weak signals (0.2 × and 0.3 × KDP for $LiCaPO_4$ and $LiNa_5(PO_4)_2$, respectively), although they consist of the same isolated PO_4 groups.

In order to determine the transparency range of $LiCs_2PO_4$, we measured the deep-UV transmittance spectrum by using a 1 mm thick crystal plate. As shown in Figure 2b, it shows a broad transparent range, and its UV cutoff edge is as short as 174 nm

DOI: 10.1021/jacs.6b06053
J. Am. Chem. Soc. 2016, 138, 9101−9104

(corresponding to a direct band gap of 7.02 eV), which is comparable to the newly developed NLO-active phosphates (Table 1). The short cutoff edge of $LiCs_2PO_4$ further demonstrates that phosphates could be good candidates for deep-UV NLO materials.

Why does $LiCs_2PO_4$ exhibit a large SHG response? We first applied the anionic group concept,[17] which suggests that macroscopic SHG behavior mainly originates from geometrical superposition of the microscopic second-order susceptibility of the NLO-active anionic groups. As shown in previous studies, the acentric distorted PO_4 groups are the dominating NLO-active units, which determine the SHG coefficients.[8] In order to quantitatively demonstrate the degree of acentric distortion of PO_4 tetrahedron, we calculated its deviation (Δd) from the idealized tetrahedral symmetry.[28] The PO_4 tetrahedra in $LiCs_2PO_4$ show a very small distortion with Δd = 0.11%, whereas the distortions of condensed PO_4 tetrahedra found in other NLO-active polyphosphates are much larger. Besides, $LiCs_2PO_4$ has the smallest number density (per unit volume) of PO_4 tetrahedra, yet the material exhibits the largest SHG response in the deep-UV NLO phosphates (Tables 1 and S4). Moreover, since the alignment of anionic groups can be influenced by cation size effect,[15] dipole moment calculations[29] were performed, which reveal that PO_4 tetrahedra have two different orientations (Table S5 and Figure S2). In $LiCs_2PO_4$, the distortion of PO_4 units is the smallest among all the phosphates discussed here, and these PO_4 units are NOT cooperatively aligned. Therefore, it is difficult to explain the large SHG response of $LiCs_2PO_4$ using the anionic group concept alone.

We performed first-principles calculations using the plane-wave pseudopotential method with the CASTEP package.[30] $LiCs_2PO_4$ is insulating with a direct band gap of 5.07 eV (Figure S3), which is substantially smaller than the experimental value of 7.02 eV (a well-known artifact of the local density approximation functional). Therefore, the "scissors" correction approximation[31] was employed. According to the *mm*2 symmetry, the calculated SHG coefficients of $LiCs_2PO_4$ are $d_{15} = d_{31} = -0.65$ pm/V, $d_{24} = d_{32} = 0.22$ pm/V, and $d_{33} = 0.61$ pm/V. Among them, d_{15} and d_{33} are approximately two times that of KDP ($d_{36}^{KDP} = 0.39$ pm/V), which agree well with the experimental powder SHG measurements. In addition, the electronic structure was calculated to explore the intrinsic relationship between the structure and optical properties (Figure 3a). As seen from the partial densities of electronic states (PDOS), the valence band (VB) near the Fermi level is mainly due to the contributions of the 2p orbitals of oxygen atoms, while the conduction band (CB) is formed primarily by the hybridization orbitals of O and P atoms and Li-1s orbital. To identify NLO-active electronic states and corresponding structural units, the so-called band-resolved method[32] was employed. Only virtual-electron (VE) process was shown and plotted at the bottom of Figure 3a because it shows dominant contribution for SHG response, about 94.7%. Similar to borate-based NLO materials,[33] the main response region is located at the narrow range (−3 to 0 eV) of VB near the Fermi level, which is almost entirely occupied by the nonbonding 2p orbitals of oxygen atoms. Therefore, these nonbonding O-2p orbitals should play the key role for the SHG response.

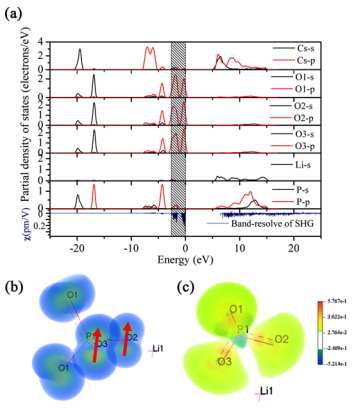

Figure 3. Electronic structure of $LiCs_2PO_4$. (a) The PDOS and band-resolved VE process; (b) the orientation of the O-2p orbital based on orbital analysis; and (c) deformation charge density map.

Next, to provide insights for the mechanism of SHG enhancement, we consider the special edge-sharing tetrahedra connectivity in $LiCs_2PO_4$. Interestingly, one can see that two nonbonding O-2p orbitals involving in the edge-sharing linkage (belong to O2 and O3 atoms) have the same direction, namely, are preferentially oriented (Figure 3b). In addition, Figure 3c gives the deformation charge density map of this compound, which reveals some differences between O1 and O2/O3 atoms in electron configurations. It also confirms that there are some degrees of covalence interaction between Li and O2/O3 atoms. More importantly, all nonbonding O2 and O3-2p orbitals have preferentially orientation along the *a* axes as a result of the edge-sharing tetrahedra connectivity (Figure S4). These aligned nonbonding O-2p orbitals may increase the microscopic second-order susceptibility, yielding the large SHG response. This phenomenon is, in some ways, very similar to the cases of large SHG response caused by "constructively aligned" stereochemically active lone-pair electrons, as observed in many NLO materials containing SOJT cations,[34] though the underlying mechanisms are different. Furthermore, the nonbonding O-2p orbitals have different directions in $LiNa_5(PO_4)_2$ and $LiCaPO_4$ (Figure S5). Although sharing similar PO_4 tetrahedra as NLO-active units, $LiNa_5(PO_4)_2$ and $LiCaPO_4$ do not exhibit any geometric structural benefit from nonbonding O-2p orbitals, and they generate a very weak SHG response. As a consequence, we can draw a conclusion that the SHG response of $LiCs_2PO_4$ originates from the geometrical superposition of the microscopic second-order susceptibility of PO_4 groups and the preferred spatial orientation of nonbonding O-2p orbitals.

In summary, we have discovered a new deep-UV transparent material, $LiCs_2PO_4$. This orthophosphate consists of regular isolated PO_4 units but produces large powder SHG efficiency of 2.6 times that of KDP. It also exhibits a very short UV cutoff edge down to 174 nm and type I phase matching behavior. This work impressively shows the innovative potential of phosphates as new NLO materials with both large SHG response and deep-UV transparency. For the first time, we captured that the SHG enhancement of $LiCs_2PO_4$ is intimately associated with its unique structural feature, i.e., the edge-sharing LiO_4-PO_4 tetrahedra and aligned nonbonding O-2p orbitals. Our future work will be devoted to uncovering the underlying relationship between SHG response and nonbonding O-2p orbitals and to the syntheses of other phases in the related systems.

■ ASSOCIATED CONTENT

Supporting Information

The Supporting Information is available free of charge on the ACS Publications website at DOI: 10.1021/jacs.6b06053.

DOI: 10.1021/jacs.6b06053
J. Am. Chem. Soc. 2016, 138, 9101−9104

Experimental methods and additional tables and figures (PDF)
Crystallographic data (TXT)

AUTHOR INFORMATION

Corresponding Authors

*krp@northwestern.edu
*slpan@ms.xjb.ac.cn

Author Contributions

‖These authors contributed equally.

Notes

The authors declare no competing financial interest.

ACKNOWLEDGMENTS

This work was supported by West Light Foundation of the CAS (grant no. 2015-XBQN-B-11), the NSFC (grant nos. 51425206, U1129301), the Xinjiang International Science & Technology Cooperation Program (20146001), the Funds for Creative Cross & Cooperation Teams of CAS, Xinjiang Key Laboratory Foundation (grant no. 2014KL009), the Science and Technology Project of Urumqi (grant 51425206), and from the National Science Foundation (awards DMR-1005827 and DMR-1307698).

REFERENCES

(1) (a) Chen, C. T.; Sasaki, T.; Li, R. K.; Wu, Y. C.; Lin, Z. S.; Mori, Y.; Hu, Z. G.; Wang, J. Y.; Gerard, A.; Masashi, Y.; Yushi, K. *Nonlinear optical borate crystals: Principals and applications*; John Wiley & Sons: Weinheim, 2012. (b) Becker, P. *Adv. Mater.* **1998**, *10*, 979−992. (c) Xia, Y. N.; Chen, C. T.; Tang, D. Y.; Wu, B. C. *Adv. Mater.* **1995**, *7*, 79−81. (d) Sasaki, T.; Mori, Y.; Yoshimura, M.; Yap, Y. K.; Kamimura, T. *Mater. Sci. Eng., R* **2000**, *30*, 1−54. (e) Yu, H. W.; Wu, H. P.; Pan, S. L.; Yang, Z. H.; Hou, X. L.; Su, X.; Jing, Q.; Poeppelmeier, K. R.; Rondinelli, J. M. *J. Am. Chem. Soc.* **2014**, *136*, 1264−1267.

(2) Huang, H. W.; Yao, J. Y.; Lin, Z. S.; Wang, X. Y.; He, R.; Yao, W. J.; Zhai, N. X.; Chen, C. T. *Angew. Chem., Int. Ed.* **2011**, *50*, 9141−9144.

(3) Wu, H. P.; Yu, H. W.; Yang, Z. H.; Hou, X. L.; Su, X.; Pan, S. L.; Poeppelmeier, K. R.; Rondinelli, J. M. *J. Am. Chem. Soc.* **2013**, *135*, 4215−4218.

(4) Wu, H. P.; Yu, H. W.; Pan, S. L.; Huang, Z. J.; Yang, Z. H.; Su, X.; Poeppelmeier, K. R. *Angew. Chem., Int. Ed.* **2013**, *52*, 3406−3410.

(5) Zhao, S. G.; Gong, P. F.; Bai, L.; Xu, X.; Zhang, S. Q.; Sun, Z. H.; Lin, Z. S.; Hong, M. C.; Chen, C. T.; Luo, J. H. *Nat. Commun.* **2014**, *5*, 4019.

(6) Zhao, S. G.; Gong, P. F.; Luo, S. Y.; Liu, S. J.; Li, L.; Adnan, M.; Khan, T.; Hong, M. C.; Lin, Z. S.; Luo, J. H. *J. Am. Chem. Soc.* **2015**, *137*, 2207−2210.

(7) Zhao, S. G.; Kang, L.; Shen, Y. G.; Wang, X. D.; Asghar, M. A.; Lin, Z. S.; Xu, Y. Y.; Zeng, S. Y.; Hong, M. C.; Luo, J. H. *J. Am. Chem. Soc.* **2016**, *138*, 2961−2964.

(8) Yu, P.; Wu, L. M.; Zhou, L. J.; Chen, L. *J. Am. Chem. Soc.* **2014**, *136*, 480−487.

(9) Li, Z. H.; Lin, Z. S.; Wu, Y. C.; Fu, P. Z.; Wang, Z. Z.; Chen, C. T. *Chem. Mater.* **2004**, *44*, 2906−2908.

(10) (a) Pan, S. L.; Wu, Y. C.; Fu, P. Z. *Chem. Mater.* **2003**, *15*, 2218−2221. (b) Pan, S. L.; Wu, Y. C.; Fu, P. Z. *J. Opt. Soc. Am. B* **2004**, *21*, 761−764.

(11) Yu, H. W.; Zhang, W. G.; Young, J.; Rondinelli, J. M.; Halasyamani, P. S. *Adv. Mater.* **2015**, *27*, 7380−7385.

(12) (a) Dmitriev, V. G.; Gurzadyan, G. G.; Nikogosyan, D. N.; Lotsch, H. K. V. *Handbook of Nonlinear Optical Crystals*; Springer: Berlin, 1999. (b) Wang, Y.; Pan, S. L.; Yu, H. W.; Su, X.; Zhang, M.; Zhang, F. F.; Han, J. *Chem. Commun.* **2013**, *49*, 306−308. (c) Wang, Y.; Pan, S. L.; Su, X.; Yang, Z. H.; Dong, L. Y.; Zhang, M. *Inorg. Chem.* **2013**, *52*, 1488−1495.

(13) (a) Kim, M. K.; Kim, S.-H.; Chang, H.-Y.; Halasyamani, P. S.; Ok, K. M. *Inorg. Chem.* **2010**, *49*, 7028−7034. (b) Yu, H. W.; Zhang, W. G.; Young, J.; Rondinelli, J. M.; Halasyamani, P. S. *J. Am. Chem. Soc.* **2016**, *138*, 88−91. (c) Yu, H. W.; Young, J.; Wu, H. P.; Zhang, W. G.; Rondinelli, J. M.; Halasyamani, P. S. *J. Am. Chem. Soc.* **2016**, *138*, 4984−4989.

(14) Shi, Y. J.; Pan, S. L.; Dong, X. Y.; Wang, Y.; Zhang, M.; Zhang, F. F.; Zhou, Z. X. *Inorg. Chem.* **2012**, *51*, 10870−10875.

(15) Zhao, S. G.; Gong, P. F.; Luo, S. Y.; Bai, L.; Lin, Z. S.; Tang, Y. Y.; Zhou, Y. L.; Hong, M. C.; Luo, J. H. *Angew. Chem., Int. Ed.* **2015**, *54*, 4217−4221.

(16) Zhao, S. G.; Gong, P. F.; Luo, S. Y.; Bai, L.; Lin, Z. S.; Ji, C. M.; Chen, T. L.; Hong, M. C.; Luo, J. H. *J. Am. Chem. Soc.* **2014**, *136*, 8560−8563.

(17) Chen, C. T.; Wu, Y. C.; Li, R. K. *Int. Rev. Phys. Chem.* **1989**, *8*, 65−91.

(18) O'Keeffe, M.; Peskov, M. A.; Ramsden, S. J.; Yaghi, O. M. *Acc. Chem. Res.* **2008**, *41*, 1782−1789.

(19) Koch, E.; Fischer, W. Z. *Z. Kristallogr. - Cryst. Mater.* **1995**, *210*, 407−414.

(20) (a) Brese, N. E.; O'Keeffe, M. *Acta Crystallogr., Sect. B: Struct. Sci.* **1991**, *47*, 192−197. (b) Brown, I. D.; Altermatt, D. *Acta Crystallogr., Sect. B: Struct. Sci.* **1985**, *41*, 244−247.

(21) (a) Sun, T. Q.; Shan, P.; Chen, H.; Liu, X. W.; Liu, H. D.; Chen, S. L.; Cao, Y. A.; Kong, Y. F.; Xu, J. J. *CrystEngComm* **2014**, *16*, 10497−10504. (b) Shan, P.; Sun, T. Q.; Chen, H.; Liu, H. D.; Chen, S. L.; Liu, X. W.; Kong, Y. F.; Xu, J. J. *Sci. Rep.* **2016**, *6*, 25201.

(22) (a) Pauling, L. *J. Am. Chem. Soc.* **1929**, *51*, 1010. (b) Huppertz, H.; von der Eltz, B. *J. Am. Chem. Soc.* **2002**, *124*, 9376−9377.

(23) Averbuch-Pouchot, M.-T.; Durif, A. *Topics in Phosphate Chemistry*; World Scientific: Singapore, 1996.

(24) (a) Kurtz, S. K.; Perry, T. T. *J. Appl. Phys.* **1968**, *39*, 3798−3813. (b) Lu, H. C.; Gautier, R.; Donakowski, M. D.; Tran, T. T.; Edwards, B. W.; Nino, J. C.; Halasyamani, P. S.; Liu, Z. T.; Poeppelmeier, K. R. *J. Am. Chem. Soc.* **2013**, *135*, 11942−11950. (c) Donakowski, M. D.; Gautier, R.; Lu, H. C.; Tran, T. T.; Cantwell, J. R.; Halasyamani, P. S.; Poeppelmeier, K. R. *Inorg. Chem.* **2015**, *54*, 765−772.

(25) Lightfoot, P.; Pienkowski, M. C.; Bruce, P. G.; Abrahams, I. *J. Mater. Chem.* **1991**, *1*, 1061−1063.

(26) Rastsvetaeva, R. K.; Khomyakov, A. P. *Crystallogr. Rep.* **1994**, *39*, 35−41.

(27) Li, L.; Han, S. J.; Lei, B.-H.; Wang, Y.; Li, H. Y.; Yang, Z. H.; Pan, S. L. *Dalton Trans.* **2016**, *45*, 3936−3942.

(28) Makovicky, E.; Balic-Žunic, T. *Acta Crystallogr., Sect. B: Struct. Sci.* **1998**, *54*, 766−773.

(29) (a) Zhang, J. J.; Zhang, Z. H.; Zhang, W. G.; Zheng, Q. X.; Sun, Y. X.; Zhang, C. Q.; Tao, X. T. *Chem. Mater.* **2011**, *23*, 3752−3761. (b) Ok, K. M.; Halasyamani, P. S. *Inorg. Chem.* **2005**, *44*, 3919−3925. (c) Maggard, P. A.; Nault, T. S.; Stern, C. L.; Poeppelmeier, K. R. *J. Solid State Chem.* **2003**, *175*, 27−31.

(30) Clark, S. J.; Segall, M. D.; Pickard, C. J.; Hasnip, P. J.; Probert, M. J.; Rrfson, K.; Payne, M. C. *Z. Kristallogr. - Cryst. Mater.* **2005**, *220*, 567−570.

(31) (a) Godby, R. W.; Schluter, M.; Sham, L. J. *Phys. Rev. B: Condens. Matter Mater. Phys.* **1988**, *37*, 10159. (b) Wang, C. S.; Klein, B. M. *Phys. Rev. B: Condens. Matter Mater. Phys.* **1981**, *24*, 3417. (c) Hybertsen, M. S.; Louie, S. G. *Phys. Rev. B: Condens. Matter Mater. Phys.* **1986**, *34*, 5390.

(32) Lee, M.-H.; Yang, C.-H.; Jan, J.-H. *Phys. Rev. B: Condens. Matter Mater. Phys.* **2004**, *70*, 235110.

(33) (a) Zhang, B. B.; Yang, Z. H.; Yang, Y.; Lee, M.-H.; Pan, S. L.; Jing, Q.; Su, X. *J. Mater. Chem. C* **2014**, *2*, 4133−4141. (b) Su, X.; Wang, Y.; Yang, Z. H.; Huang, X. C.; Pan, S. L.; Li, F.; Lee, M.-H. *J. Phys. Chem. C* **2013**, *117*, 14149−14157.

(34) (a) Chang, H.-Y.; Kim, S.-H.; Halasyamani, P. S.; Ok, K. M. *J. Am. Chem. Soc.* **2009**, *131*, 2426−2427. (b) Cheng, W. D.; Lin, C. S.; Luo, Z. Z.; Zhang, H. *Inorg. Chem. Front.* **2015**, *2*, 95−107.

DOI: 10.1021/jacs.6b06053
J. Am. Chem. Soc. 2016, 138, 9101−9104